

# Nonstationary behaviour of partial discharge during discharge induced ageing of dielectrics

R.J. Van Brunt  
P. von Glahn  
T. Las

*Indexing terms:* Ageing, Epoxy, Partial discharge, Point-electric gaps, Stochastic behaviour, Surface conductivity

**Abstract:** Changes in the stochastic behaviour of pulsating partial discharge with time have been observed when an alternating voltage is applied to point-dielectric gaps in which the dielectric is a cast epoxy resin either with, or without,  $\text{Al}_2\text{O}_3$  filler. The changes in discharge behaviour are shown, with the help of a Monte-Carlo simulation, to be consistent with discharge induced increases in the surface conductivity of the epoxy. This 'ageing' effect is shown to be accelerated as the frequency of applied voltage is increased from 50 to 800 Hz. The implications of the results on accelerated ageing tests and definition of partial discharge 'signatures' for possible pattern recognition are discussed. The relationship between average partial discharge current and partial discharge pulse height distributions is also discussed.

## 1 Introduction

Investigations have been under way in a number of laboratories to relate the observed statistical characteristics of partial discharge (PD) to properties of the site at which the discharge occurs [1-6]. There is an expectation that the statistical characteristics of PD can provide information needed for insulation defect site identification [7-12]. The success of PD identification schemes depends on finding a sufficiently complete set of defect site descriptors to allow assignment of unique, meaningful PD signatures to these sites. Special difficulties are encountered in cases where PD induced ageing occurs (i.e. where there are physical and chemical changes at the discharge site that, in turn, cause modifications in the statistical characteristics of the PD).

There is experimental evidence that the statistical behaviour of PD will change with time owing to discharge induced changes in the insulating characteristics of a dielectric [13-15]. Of particular relevance in the present work is the case where the occurrence of PD causes a change in the conductivity of a dielectric surface which, in turn, changes the discharge characteristics. This case was first investigated in 1958 by Rogers [16] who showed that the 'self-extinction' of pulsating PD in a

dielectric cavity can be attributed to a discharge induced increase in the conductivity of the cavity walls. More recently, Hudon and coworkers [17] have been able to relate the transition of a pulsating discharge into a glow discharge in a gap formed by parallel epoxy resin planes to a discharge induced increase in the epoxy surface conductivity. Changes in discharge behaviour associated with changes in the electrical characteristics of solid dielectric materials during operation of the discharge have also recently been investigated by Morshuis [18] and T. Ishida and coworkers [19]. The present work provides additional evidence for PD induced changes in epoxy surface resistivity and relates these changes to observed nonstationary behaviour in the statistical characteristics of the PD with the aid of a previously described Monte-Carlo simulator [20, 21].

The observed nonstationary behaviour of PD pulses, manifested by a time dependence in their statistical characteristics, illustrates the difficulties to be encountered in defining meaningful PD pulse 'patterns' that can be used for reliable defect site identification. The experimental results presented here prove the necessity of considering ageing effects in defining the characteristics of a discharge site. It will be argued that it is generally not sufficient to specify only the dielectric material, gap (or void) geometry, and gas content in the gap in making meaningful connections between discharge behaviour and gap characteristics. Additional information such as the time dependent surface conductivity of dielectric materials in the discharge gap is also needed.

The frequency dependence of discharge induced ageing of the dielectric surface in point-dielectric gaps has also been investigated in the present work; and the implications of the results on accelerated ageing tests are discussed. Possible difficulties in relating measured PD

This work was performed in the Electricity Division, Electronics & Electrical Engineering Laboratory, National Institute of Standards & Technology, Technology Administration, US Department of Commerce. Partial support was received from the Office of Energy Storage and Distribution, Electric Energy System Program, US Department of Energy and from the Nuclear Regulatory Commission. Support was also provided for participation of the Electrotechnical Institute in Warsaw, Poland through the Maria Skłodowska-Curie Joint Fund, US-Polish Joint Commission. The authors are grateful for assistance provided by E.W. Cernyar.

© IEE, 1995

Paper 1435A (S3), first received 3rd March and in revised form 7th June 1994

R.J. Van Brunt and P. von Glahn are with the National Institute of Standards and Technology, Gaithersburg, MD 20899, USA

T. Las is with the Electrotechnical Institute, Warsaw, Poland



pulse-height distributions to measured average PD current that are relevant to the calibration of PD measurement systems are also discussed. Preliminary reports of the work covered here have been given previously [22, 23].

## 2 Measurements

The experimental results were obtained for an alternating sinusoidal voltage of variable frequency applied to a point-dielectric gap configuration described previously [21, 24]. Partial discharge was generated under conditions where a conical stainless-steel 'point' electrode with a radius of curvature at the tip of about 0.05 mm either touched or was slightly displaced from the flat surface of a square 8 × 8 cm sheet of 2.0 mm thick epoxy attached to a grounded metal surface in air. A diagram of the discharge gap is shown in Fig. 1. Results are presented here

Sources of error in the measurement of  $Q^+$  and  $Q^-$  are discussed [25]. Because  $|\langle q_i^+ \rangle| > |\langle q_i^- \rangle|$  for the cases considered here, the error in  $Q^-$  tends to be greater than that in  $Q^+$ , but is expected to be less than  $\pm 20\%$ .

After exposure to PD, surface resistivities of the epoxy were measured in the region where the discharge had occurred. These measurements were made by recording the current produced when a DC voltage was applied to movable parallel conductors separated by a distance of 1.0 mm as shown in Fig. 2. The resistances were measured as a function of the distance  $d'$  from the centre of the discharge site.

In some cases the average PD currents,  $I_m$  were also measured under the same gap and operating voltage conditions in separate experiments. These measurements were performed using a Tettex-9120 PD measurement system.\* The results from the  $I_m$  measurements are compared with the average currents predicted from the measured integrated charge distributions.

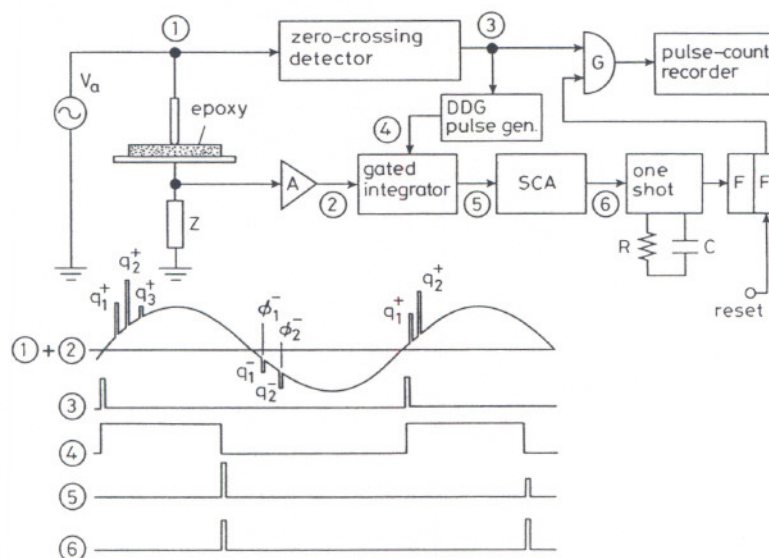


Fig. 1 Experimental arrangement showing circuit used to measure number of cycles to extinction of positive PD pulses ( $n_p$ )

Specific circuit elements include: G, gate; DDG, digital delay generator; SCA, single-channel analyser; A, amplifier; and FF, flipflop. Also shown is pulse-timing diagram corresponding to signals that appear at different indicated locations in circuit

for point-to-plane gaps  $d$  of 0.0 (point touching the dielectric) and 0.5 mm (point slightly displaced from the dielectric). Two types of cast epoxy (with and without  $\text{Al}_2\text{O}_3$  'filler') supplied by the Electrotechnical Institute in Warsaw were used in this investigation. Preliminary results were also obtained for pure  $\text{Al}_2\text{O}_3$  samples. For the data reported here, the applied sinusoidal voltage was always 3.0 kV RMS and the frequency was set to a value in the range of 50 to 800 Hz.

During continuous application of the voltage, various conditional and unconditional PD pulse height, pulse phase, and integrated charge distributions were measured with a stochastic analyser [21, 26]. Results are reported here for the unconditional phase of occurrence distributions for the first negative PD pulse  $p_0(\phi_1^-)$  and for the integrated charge distributions,  $p_0(Q^+)$  and  $p_0(Q^-)$ , where  $Q^+$  and  $Q^-$  are, respectively, the sums of charges  $q_i^\pm$  in pC of all positive or negative PD pulses in one cycle of the applied voltage, i.e.

$$Q^\pm = \sum_i q_i^\pm \quad (1)$$

As will be shown in the next Section, positive PD pulses were found to disappear under certain conditions at a particular time after the voltage was applied. A special circuit shown in Fig. 1 was set up to measure the number of cycles  $n_p$ , or equivalently the time  $t_p$ , from the beginning of the discharge to cessation of the positive PD pulses. A pulse-timing diagram for the circuit is also shown in Fig. 1. The circuit allows pulses generated by a zero-crossing detector to be counted and displayed by the pulse-count recorder provided the gate G is held open by the output of flipflop FF. The flipflop is set to open gate G at the reset input when the voltage is first applied to the gap. The output of the zero-crossing detector is also used to trigger a digital delay generator (DDG) which controls the operation of a gated integrator. The integrator produces an output pulse with an amplitude pro-

\* The identification of commercial instruments and their sources is made to describe the experiment adequately. This neither implies recommendation by the National Institute of Standards and Technology, nor that the instrument is the best available.



portional to  $Q^+$  which is the sum of the amplitudes of all positive pulses that occur in a phase window defined by the DDG pulse. The integrator pulse triggers a single-

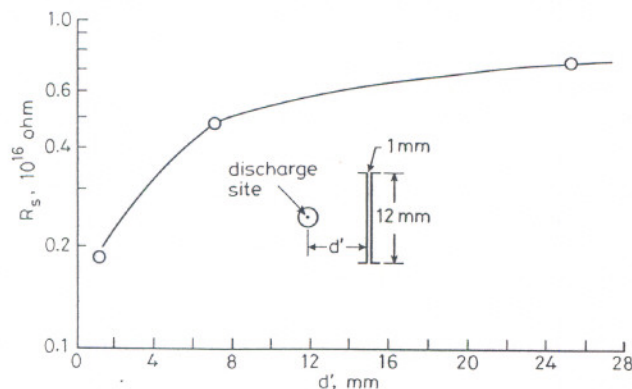


Fig. 2 Measured surface resistance of epoxy with filler as function of distance from discharge site

These results apply to data shown in Fig. 3

channel analyser (SCA) which, in turn, triggers a retriggerable monostable multivibrator (one shot). The lower discrimination level of the SCA defines the minimum integrated charge that will produce an output pulse to trigger the one shot. This level was set at 10 pC or lower which is far below the typical initial mean of the positive integrated charge (see Fig. 3). The output of the

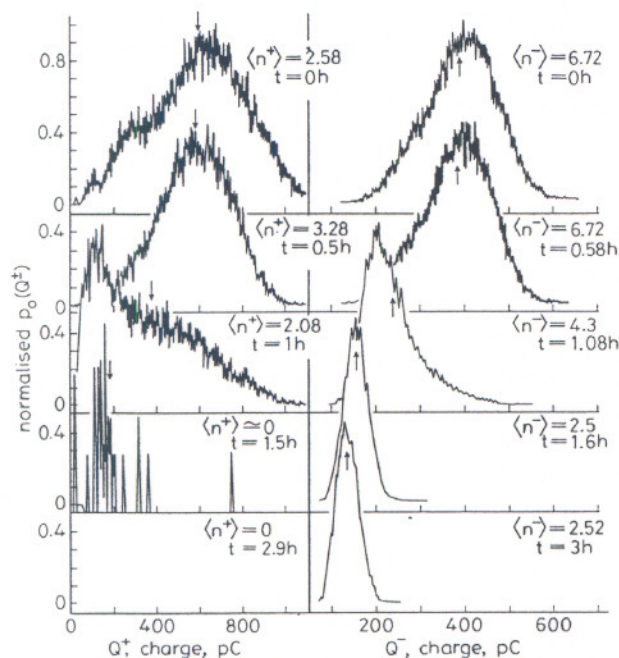


Fig. 3 Positive and negative integrated charge distributions measured for epoxy with  $\text{Al}_2\text{O}_3$  filler and  $d = 0.0$  mm at indicated times after 50 Hz voltage was applied

Also shown are corresponding mean numbers of positive and negative PD pulses per cycle and mean charge values (vertical arrows)

one shot will cause the flipflop to change state and thus close G only if the gated integrator does not produce a pulse in a time less than the RC constant of the one shot. The time-constant value is selected to be much greater than the period  $T$  of the applied voltage. The results reported here were obtained with  $RC = 1.11 \pm 0.05$  s [i.e. the positive pulses were assumed to have ceased if the integrated positive charge failed to exceed the SCA

threshold within  $(1.11 \pm 0.05)/T$  cycles]. Detailed descriptions of the gated integrator and SCA are given elsewhere [26].

### 3 Experimental results

#### 3.1 Integrated charge distributions

The distributions  $p_0(Q^+)$  and  $p_0(Q^-)$  were measured at different times during a continuous application of an alternating voltage to the point-dielectric gap. The time required for the measurement of each distribution was about 4 minutes. An example of a set of distributions measured at 50 Hz for epoxy with filler and  $d = 0.0$  mm is shown in Fig. 3 together with corresponding information about the times at which measurements were performed and the mean numbers of positive and negative discharge pulses per cycle ( $\langle n^+ \rangle$  and  $\langle n^- \rangle$ ). The mean charge values defined by

$$Q_{av}^{\pm} = \frac{\int_0^{\infty} Q^{\pm} p_0(Q^{\pm}) dQ^{\pm}}{\int_0^{\infty} p_0(Q^{\pm}) dQ^{\pm}} \quad (2)$$

are indicated in the Figure by vertical arrows. The distributions have been normalised to their maximum values.

Initially (at  $t = 0.0$  h), there is, within the measurement uncertainties, an approximate charge balance (i.e.  $|Q_{av}^+| \approx |Q_{av}^-|$ ). After the voltage has been applied for about an hour, the statistical characteristics of the discharge change dramatically. About 1.7 h, the positive PD pulses cease entirely and  $|Q_{av}^-|$  shifts to a lower value.

Fig. 4 shows an example of a set of measured positive and negative integrated charge distributions for epoxy

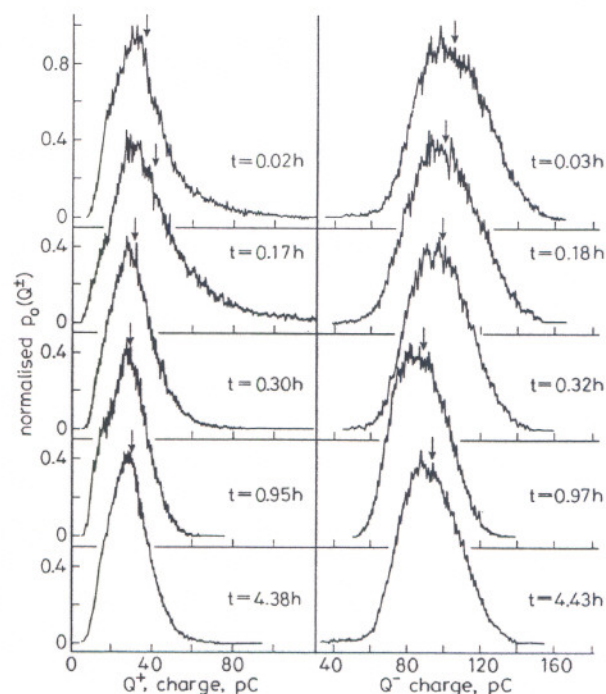


Fig. 4 Positive and negative integrated charge distributions measured for epoxy without filler and  $d = 0.0$  mm at indicated times after 400 Hz voltage was applied

Vertical arrows indicate mean charge values

without filler at different times after a 400 Hz voltage was applied. These results were obtained under conditions where the point touched the epoxy surface. Again, the vertical arrows in the Figure correspond to mean charge



values. In this case, there is an absence of charge balance from the beginning of discharge activity with  $|Q_{av}^-| > |Q_{av}^+|$  for all  $t > 0$ . Both  $|Q_{av}^-|$  and  $|Q_{av}^+|$  are seen to shift to lower values as time of discharge increases. The positive discharge pulses did not cease for this material.

Examples of results obtained in a case where there was a finite gap spacing are shown in Fig. 5. In this particular

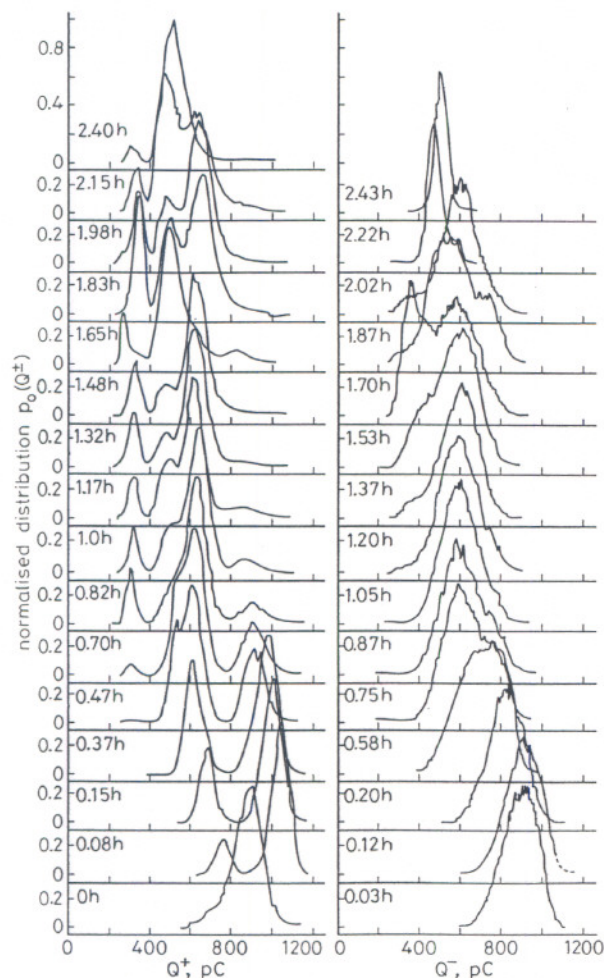


Fig. 5 Positive and negative integrated charge distributions measured for epoxy with filler and  $d = 0.5$  mm at indicated times after 200 Hz voltage was applied

case, the measurements were made using epoxy with filler with a point-to-plane gap spacing of 0.5 mm and a frequency of 200 Hz. An approximate charge balance was maintained at all times under these conditions, although both  $|Q_{av}^+|$  and  $|Q_{av}^-|$  tend to decrease with time. The multi-peaked structure in  $p_0(Q^+)$  can be understood, and have been shown previously [21] to result from the relative contributions to the distribution from cycles in which different numbers of pulses occur, i.e.

$$p_0(Q^+) = \sum_i w_i p_i(Q^+ | i) \quad (3)$$

where  $w_i p_i(Q^+ | i)$  is the probability that the positive integrated charge will have a value  $Q^+$  if  $i$  pulses occur in a half-cycle.

It should be noted that the stochastic properties of PD in point-dielectric gaps have been shown to be very sensitive to changes in the gap spacing [25]. A detailed discussion of the dependence of PD behaviour on gap spacing goes beyond the scope of the present work. The results shown in Fig. 5 serve to illustrate, however, that

the stochastic behaviour can change considerably as the geometrical configuration of the gap is changed, thus pointing to a question about one's ability to define a gap geometry precisely enough for it to be related to a specific discharge pattern.

### 3.2 Phase distributions

It has been shown in previous work that, for point-dielectric gaps, a negative correlation generally exists between  $\phi_1^-$  and  $Q^+$  [21, 24, 26]. Negative correlations are also usually found between  $\phi_1^-$  (or  $\phi_1^+$ ) and  $Q^+$  (or  $Q^-$ ) for all  $i \geq 1$ . This means that the mean phase of the first negative PD pulse  $\langle \phi_1^- \rangle$  will decrease as  $Q_{av}^+$  increases. The random variables  $\phi_1^-$  and  $Q^+$  are therefore not independent and are related by the integral expression

$$p_0(\phi_1^-) = \int_0^\infty p_0(Q^+) p_1(\phi_1^- | Q^+) dQ^+ \quad (4)$$

where  $p_1(\phi_1^- | Q^+)$  is a conditional distribution function [21, 26]. The dependence of  $\phi_1^-$  on  $Q^+$  arises because of memory effects; in particular, the influence of charge deposited on the dielectric by PD in a given half-cycle on the local electric-field strength in the gap at the time of the subsequent half-cycle [21].

It is therefore expected that, if there is a significant change in  $Q_{av}^+$  such as indicated by the results shown in Fig. 3, there should be a corresponding shift in  $\langle \phi_1^- \rangle$ . Fig. 6 shows examples of normalised phase distributions

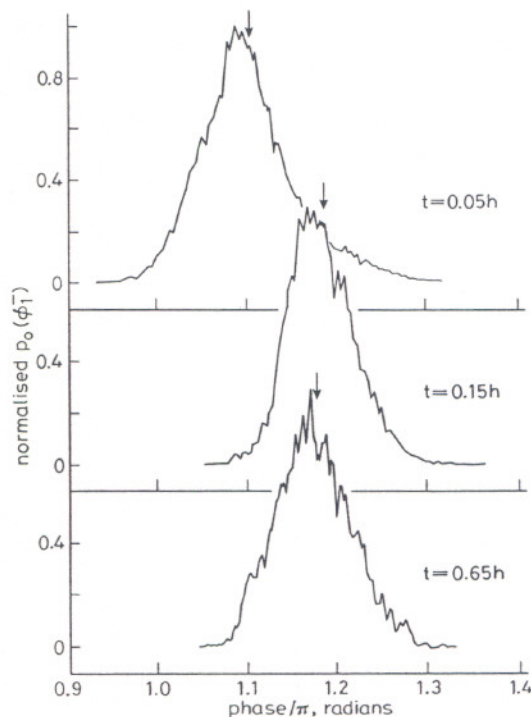


Fig. 6 Measured phase of occurrence distributions of first negative PD pulse for epoxy with filler and  $d = 0.0$  mm at indicated times after 400 Hz voltage was applied

Vertical arrows indicate mean phase values; positive PD activity ceased for  $t \geq 0.12$  h

$p_0(\phi_1^-)$  of the first negative PD pulse measured at different indicated times for epoxy with filler at a frequency of 400 Hz. In this case, the data were obtained for  $d = 0.0$  mm. When the positive discharges cease at



$t \approx 0.12$  h, the mean of  $\phi_1^-$  shifts to a value closer to the voltage minimum on the negative half-cycle as expected.

### 3.3 Frequency dependence

Shown in Figs. 7A and 7B are, respectively, the number of cycles  $n_p$ , that occur from initiation of the discharge to

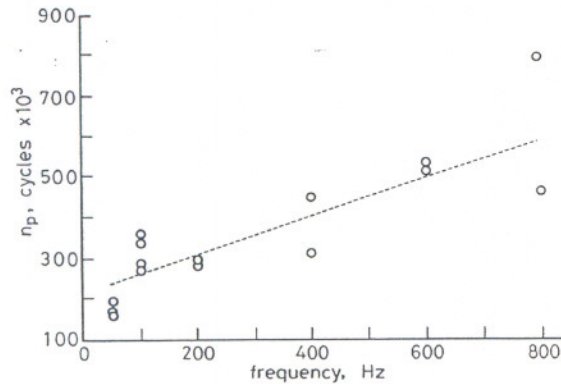


Fig. 7A Recorded number of cycles to extinction of positive PD ( $n_p$ )  
Measurements were performed for epoxy with filler and  $d = 0.0$  mm; dotted lines are fits to data

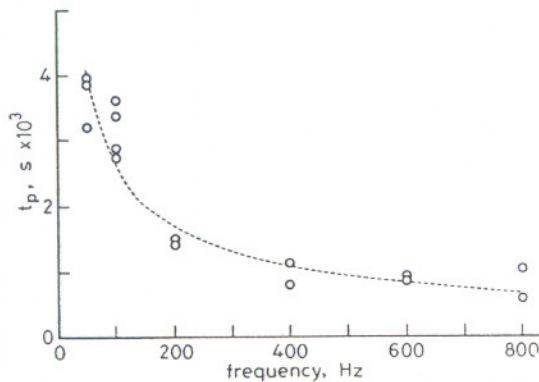


Fig. 7B Corresponding time to extinction versus frequency of applied voltage

Measurements were performed for epoxy with filler and  $d = 0.0$  mm; dotted lines are fits to data

cessation of the positive PD and the corresponding time  $t_p$  measured with the system shown in Fig. 1, where  $t_p = n_p T$ . These results were obtained for  $d = 0.0$  mm using epoxy with filler. The measurements were made at different widely separated locations on two different epoxy samples. Each point in the Figure corresponds to a single measurement made at one location on an epoxy sample, and the dotted lines are fits to the data.

The number of cycles to positive PD extinction has an approximate linear increase with frequency ( $f = 1/T$ ) given by

$$n_p \approx 2.14 \times 10^5 + 471.4f \quad (5)$$

which implies that  $t_p$  has a frequency dependence of the form  $(Af^{-1} + B)$ , where  $A$  and  $B$  are constants. In eqn. 5,  $f$  has units of inverse seconds. It was found (see dashed curve in Fig. 7B) that  $t_p$  can also be satisfactorily represented by an exponential form

$$t_p = 5.04 \times 10^4 f^{-0.643} \quad (6)$$

where  $t_p$  has units of seconds. It must be emphasised that the frequency dependence reported here in eqns. 5 and 6 applies only to the limited range of  $f$  considered and to

the restricted test conditions that were used. It was found, for example, that the time to cessation of PD pulses depends significantly on applied voltage and the shape of the point electrode. The significant aspect of the data shown in Fig. 7B is that  $t_p$  is not directly proportional to  $f^{-1}$ . As will be discussed in Section 5, frequency dependences for  $t_p$  of the forms  $(Af^{-1} + B)$  or  $f^{-\alpha}$ , with  $0 < \alpha < 1.0$ , are consistent with expectations based on the statistical behaviour of PD initiation. However, no attempt was made here to attribute physical significance to the adjustable parameters used to obtain the fits represented in eqns. 5 and 6.

### 3.4 Surface resistivity

In the case of the epoxy sample with filler used to obtain the data in Fig. 3, measurements were also made of the surface resistance near the discharge site after the sample had been exposed to the discharge for 3 hours. The results in Fig. 2 indicate that exposure to PD results in a local decrease of epoxy surface resistivity consistent with results reported by Hudon and coworkers [17]. The relative drop in surface resistivity at the discharge site was found to increase with increasing time of exposure to PD. It will be shown in the next Section that the disappearance of positive PD pulses can be related to the decrease in surface resistivity. Relative resistivity measurements were also made on many other epoxy samples before and after exposure to PD, and all showed a significant decrease in resistance near the discharge site.

Although the absolute surface resistance measurements are subject to considerable uncertainty owing to uncontrollable factors such as adsorbed moisture content, the observed changes before and after exposure to the discharge are considered to be significant. The primary purpose of these measurements was not to make precise determinations of resistance, but rather to verify previously observed trends reported by others. [17]

### 3.5 Average PD current

According to the previous IEC Standard 270 [27], the average PD current  $I_m$  is given by

$$I_m = \langle (|q_1^\pm| + |q_2^\pm| + \dots) \rangle f \quad (7)$$

where an average is performed over many cycles and  $|q_i^\pm|$  is the absolute value of the  $i$ th PD pulse amplitude to occur in a cycle expressed in pC. If there is a discharge current component  $I_b$ , not accounted for by the PD pulses, eqn. 1 should be replaced by

$$I_m = \langle (|q_1^\pm| + |q_2^\pm| + \dots) \rangle f + I_b \quad (8)$$

In general, the total charge associated with a PD pulse is given by

$$q_i^\pm = \int_{\Delta\tau} I_i^\pm(t) dt \quad (9)$$

where  $I_i^\pm(t)$  is the instantaneous PD current and the integration is over the duration  $\Delta\tau$  of the PD pulse. The conditions under which PD pulse amplitude is a measure of total charge has been covered elsewhere [28]. In particular, the amplitude is approximately proportional to charge only if the width of the impulse response of the measurement circuit is much larger than the intrinsic width of a PD pulse. The correction term  $I_b$  in eqn. 8 can include both contributions to the current from a pulse not accounted for by measuring the pulse amplitude and contributions from a pulseless component of the discharge such as might be associated with a 'glow' [17, 29].



Using eqns. 1 and 2, the contribution to the current from measurable PD pulses is given by

$$I_c = (|Q_{av}^+| + |Q_{av}^-|)f \quad (10)$$

assuming that  $|Q_{av}^+|$  and  $|Q_{av}^-|$  correspond to mean net positive and negative charges per cycle. This equation is valid for data on integrated charge reported here only if there are no 'null' half-cycles in which either no pulses occur or the total charge is below the detection threshold. This is a consequence of an error in the measurement of the distribution  $p_0(Q^\pm)$  by the present system which necessarily excludes values of  $Q^\pm$  that are below a preset discrimination level (i.e. contributions from 'zero' values associated with null half-cycles are not included). An exclusion of null cycles causes an overestimation of the mean integrated charge using eqn. 2. The error due to exclusion of null cycles can be overcome by continuously recording PD data for every cycle to determine  $|Q_{av}^+|$  and  $|Q_{av}^-|$ . This has recently been done using a new digital PD data recorder [30]. With this system, we have shown that, under conditions like those that yielded the results in Fig. 3, null positive half-cycles randomly occur at times before the positive PD cease [30].

Even if null half-cycles are properly included in the determination of  $p_0(Q^\pm)$ ,  $I_c = I_m$  only if it can be assured that  $I_b = 0$ . Moreover, the existence of a charge imbalance for PD in a point-dielectric gap ( $|Q_{av}^+| \neq |Q_{av}^-|$ ) would imply that  $I_b \neq 0$  (i.e. there must be a component of the discharge current that is not accounted for in the pulses). This follows from the requirement of charge conservation. The condition  $I_b \neq 0$  could occur, for example, if there were a loss of dielectric surface charge due to surface conduction or if part of the discharge activity occurs in a pulseless glow mode.

Fig. 8 shows a comparison of  $I_c$  and  $I_m$  for conditions similar to those used to obtain the results shown in Fig.

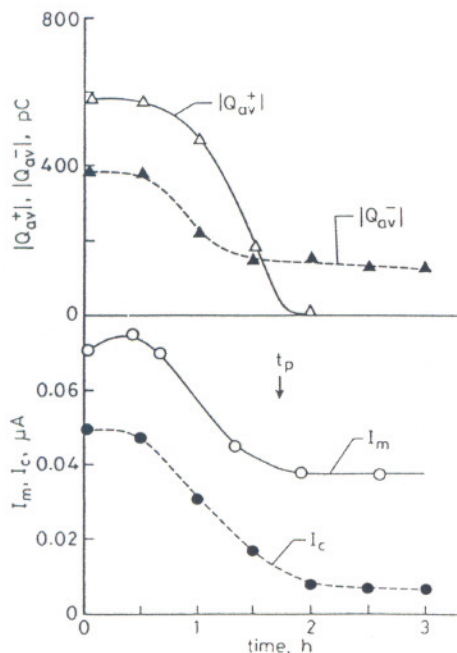


Fig. 8 Time dependencies of mean values for positive and negative integrated charges determined from measured  $p_0(Q^\pm)$  such as shown in Fig. 3 using eqn. 2 and measured  $I_m$  and calculated  $I_c$  average PD current. Indicated is time  $t_p$  at which the positive PD pulses ceased

3. Also shown in Fig. 8 are the corresponding values for  $|Q_{av}^+|$  and  $|Q_{av}^-|$ . The  $I_m$  values were obtained using the commercial PD measurement system previously men-

tioned in Section 2. It is seen that, although the curves for  $I_m$  and  $I_c$  have the same shape,  $I_m$  is always greater than  $I_c$  thus implying that  $I_b \neq 0$ . There is evidence in this case [30] that the initial charge imbalance ( $|Q_{av}^+| > |Q_{av}^-|$ ) is significant and could be explained by the above noted failure to include null half-cycles in the measurement of  $p_0(Q^\pm)$ .

#### 4 Results of Monte-Carlo simulation

The stochastic properties of PD generated by applying an alternating voltage to a point-dielectric gap can be predicted using a Monte-Carlo computer simulation previously described [20, 21]. The simulation produces a continuous, phase correlated sequence of PD pulses that is then subjected to a stochastic analysis. The physical model upon which the simulation is based is most applicable to the case where the point electrode touches the dielectric surface. The model used to obtain the present results is a modified version of the earlier model [20] (see Appendix 7) that allows for a decay of PD deposited negative charge on the dielectric surface by a factor  $\exp(-\gamma t)$ , where the decay constant  $\gamma$ , which has units of inverse seconds, increases with increasing local surface conductivity. The present model also allows the probability of extracting an initiatory electron from the negatively charged surface to increase with increasing negative-charge density. By incorporating both of these features into the model, it is possible to simulate conditions under which positive PD pulses will disappear with increasing surface conductivity as illustrated in Fig. 9. This Figure shows two randomly selected cycles of a 50 Hz applied voltage and corresponding local field at the PD site for three different assumed values of  $\gamma$ . In this example, positive PD pulses cease when  $\gamma > 150 \text{ s}^{-1}$ . Also, the mean value for the phase of the first negative pulse ( $\langle \phi_1^- \rangle$ ) increases when the positive PD pulses cease. This trend is consistent with the data in Fig. 6.

Shown in Fig. 10 are the mean numbers of positive and negative PD pulses per cycle ( $\langle n^+ \rangle$  and  $\langle n^- \rangle$ ) and the ratio of mean values for  $Q^+$  and  $Q^-$  determined from this simulation as a function of  $\gamma$ . It is seen that  $\langle n^- \rangle$  initially decreases with increasing  $\gamma$  in the region where  $\langle n^+ \rangle \rightarrow 0$  which is consistent with the data for  $\langle n^- \rangle$  in Fig. 3. However, the experimental results suggest that increases in the effective  $\gamma$  are not large enough to cause an observable increase in  $\langle n^- \rangle$  such as predicted by the model for  $\gamma > 300 \text{ s}^{-1}$ . The corresponding drop in measured  $|Q_{av}^-|$  indicated by the vertical arrows in Fig. 3 is associated with the drop in  $\langle n^- \rangle$ . In the case of the simulation results, however, the drop in  $\langle n^- \rangle$  was not great enough to cause a significant change in  $|Q_{av}^-|$ . Conditions closer to those observed experimentally can be obtained by varying the model parameters such as surface work functions and applied voltage. It should be noted that no attempt was made here to use the simulator results to fit the experimental data. The simulator parameters were only adjusted to yield results that are consistent with the experimentally observed trends for the purpose of gaining insight into the physical bases for the changes in stochastic behaviour.

It is interesting to point out that the drop in  $\langle n^+ \rangle$  becomes evident as soon as  $\gamma$  assumes a value equal to, or greater than, that for the frequency of the applied voltage, in this case  $50 \text{ s}^{-1}$ . In general, if  $\gamma > 0$ , the model will yield a charge imbalance ( $|Q_{av}^+| < |Q_{av}^-|$ ). As discussed in the previous Section, this imbalance is expected



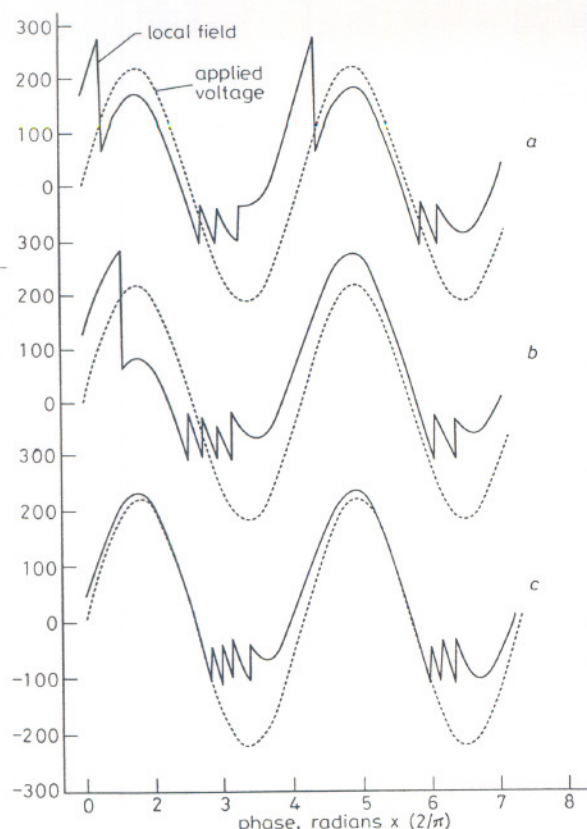


Fig. 9 Two successive randomly selected cycles from Monte-Carlo simulation of PD for each set of indicated conditions

Shown are applied sinusoidal voltage (dashed lines) and local field (solid line) at discharge site; indicated below are decay constant  $\gamma$  in units of  $\text{s}^{-1}$ , and mean values of  $\phi_1^+$  and  $Q^-$

a  $\gamma = 0.0 \text{ s}^{-1}$   $\langle \phi_1^+ \rangle = 1.066\pi$   $|Q_{av}^+| = 100.8$   
 b  $\gamma = 100 \text{ s}^{-1}$   $\langle \phi_1^+ \rangle = 1.122\pi$   $|Q_{av}^+| = 103.8$   
 c  $\gamma = 250 \text{ s}^{-1}$   $\langle \phi_1^+ \rangle = 1.117\pi$   $|Q_{av}^+| = 115.9$

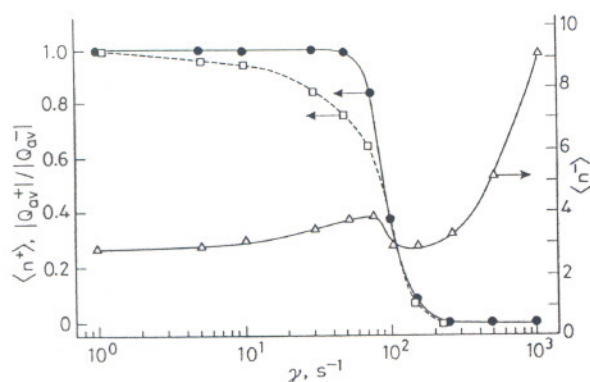


Fig. 10 Dependencies of mean numbers of positive and negative PD pulses ( $\langle n^+ \rangle$  and  $\langle n^- \rangle$ ) and ratio of mean absolute integrated charge values  $|Q_{av}^+|/|Q_{av}^-|$  on assumed decay constant predicted by Monte-Carlo simulation

●  $\langle n^+ \rangle$     △  $\langle n^- \rangle$     □  $|Q_{av}^+|/|Q_{av}^-|$

because a finite value for  $\gamma$  implies the existence of a component of the discharge current not included in the PD pulses.

## 5 Discussion and conclusions

Consistent with the results reported by others [17], it was found here that the surface conductivity of cast

epoxy resin materials is increased when exposed to partial discharge activity. Also consistent with previous observations [16, 17], it was discovered that the discharge induced changes of the dielectric surface modify the statistical behaviour of PD and may even cause a cessation of the pulsating characteristic. In the case of epoxy with  $\text{Al}_2\text{O}_3$  filler, it was found that the pulses which occur on the positive half-cycle will extinguish after the discharge has been active for a certain period of time. The time to positive PD pulse extinction was found to decrease with increasing frequency.

The precise nature of the physical and chemical changes in the surface that give rise to a local decrease in surface resistivity are not yet understood. When filler is present, the decrease in resistivity may be associated, at least in part, with an enrichment in the  $\text{Al}_2\text{O}_3$  content of the surface. Preliminary measurements made with 'pure'  $\text{Al}_2\text{O}_3$  samples revealed that positive PD pulses failed to occur even at the time that the voltage was first applied to the gap. In the case of epoxy without  $\text{Al}_2\text{O}_3$  filler (see Fig. 4), the positive PD activity did not cease under the conditions considered here, although shifts were observed in the mean values of integrated charge that suggest modification of the surface conductivity. Subsequent measurements of the relative surface resistance after exposure to the discharge revealed decreases near the discharge site independent of whether or not the filler material was present. However, the pure cast epoxy resin samples without filler tend to exhibit smaller changes in surface resistivity and a lower initial resistivity. A lower initial surface resistivity would be consistent with the data in Fig. 4 that show a net charge imbalance ( $|Q_{av}^-| > |Q_{av}^+|$ ) that occurs even at the start of discharge activity. There is evidence from the work of Hudon and coworkers [31] that droplets of glycolic and formic acid also appear on epoxy surfaces exposed on discharges. These acids are known to be far more conductive than the epoxy resin matrix [17, 31]. In support of the hypothesis that decreases in surface resistivity are predominantly due to deposits, it was observed that, in most cases, the surface resistivity could be restored nearly to its pre-discharge value by subsequent 'cleaning' of the surface with a damp cloth. More investigations of the discharge induced surface modifications will be required before the changes in surface resistivity can be fully understood.

With the aid of a Monte-Carlo simulator, it has been possible to show that a net charge imbalance, and the eventual disappearance of positive PD pulses, is consistent with an increase in dielectric surface conductivity. To do this, the physical model upon which the simulation is based [20, 21] had to be modified to allow for a decay of negative charge at the discharge site associated with a finite surface conductivity. The present model assumes that there is no decay of positive charge (i.e. the positive charge carriers remain in place during times comparable to or greater than the period of the applied voltage). This assumption is supported by measurements that were performed of the epoxy surface charge after exposure to PD using an electrostatic probe. These measurements showed that there was a quasipermanent residual positive charge that remained on the surface after the discharge was turned off. It was quasipermanent in the sense that it could be removed by wiping the surface with a damp cloth.

An additional assumption was required to allow for a complete disappearance of positive PD, namely that the probability for the initiation of a positive PD pulse increases with increasing density of negative surface



charge. This is considered to be a physically reasonable assumption which means that the probability for ejection of an initiatory electron from a surface will be proportional to the number of excess electrons trapped at the surface when the local field changes sign in going from negative to positive half-cycles. It is particularly significant to note that the model predicts a charge imbalance between positive and negative PD whenever charge is allowed to leak away from the discharge site. Measurement of the changes in charge imbalance could thus be an indicator of changes in local surface conductivity.

The disappearance of positive PD can be used as a reference point to define a specific level of discharge induced 'ageing' of the dielectric material. The time required for the extinction of positive pulses is associated with the time required for the material to reach a particular state of modification manifested here by a critical level of the surface conductivity attained during the occurrence of PD. The results on the frequency dependence shown in Fig. 7 have significant implications on the design and interpretation of 'accelerated ageing' tests in which the acceleration is achieved by increasing the frequency of the applied voltage. It was found here that the number of cycles required to reach positive PD extinction does not remain constant with frequency and increases as the frequency increases. Correspondingly, the time to extinction does not decrease in direct proportion to  $1/f$ . In fact,  $t_p$  increases more slowly than  $1/f$  and is nearly independent of frequency for  $f > 400$  Hz. The dependence of ageing rate on frequency observed here can be understood in terms of the frequency dependent stochastic behaviour of the discharge. It was found, both from measurements and simulations based on the Monte-Carlo model that, when the frequency of the applied voltage is increased and all other parameters are held constant, there will be a decrease in the mean number of PD pulses per cycle. This is merely a consequence of the fact that there is less time available in a particular phase interval for the initiation of a discharge pulse (i.e. the probability for initiation of a PD at any point in the cycle decreases with increasing rate-of-change of the instantaneous voltage). If fewer pulses per cycle means a slower rate of ageing, it can be expected, as observed here that, with an increase in  $f$ , there will be an increase in the number of cycles required to reach a particular level of discharge induced ageing. Although it was found that the ageing effect observed here could be approximately simulated by allowing the dielectric surface conductivity (or equivalently  $\gamma$ ) to increase with time in proportion to the accumulated PD exposure (measured by total negative charge), more work will be required to determine if this can yield the proper frequency dependence and if there is a physical basis for the assumed ageing mechanism.

The results of the measured integrated charge and phase of occurrence distributions shown here in Figs. 3–6 indicate the difficulties that can be encountered in attempting to define meaningful signatures based on the statistical behaviour of PD for possible use in pattern recognition schemes. It has previously been argued that it should be possible to use phase resolved PD pulse height information to identify the geometrical characteristics of a 'defect' site at which the PD occur [4]. This assertion is based on an assumption that there is a unique statistical behaviour that can be assigned to a particular geometrical configuration. The results presented here show that this is generally not possible. Information about the geometrical configuration alone is not sufficient to determine the statistical characteristics of a discharge that occurs at

a particular site. Information about other properties of the site are also required such as dielectric surface conductivity.

The present results also clearly demonstrate that PD can exhibit significant nonstationary behaviour manifested by a time dependence of measured statistical distributions such as the integrated charge distributions  $p_0(Q^+)$  and  $p_0(Q^-)$ . This poses an additional problem in defining patterns based on statistical data. In general, it may be necessary to consider the time development of the discharge in defining patterns as previously suggested [21].

Finally, it should be noted that the results of the present work also point to the difficulties in relating PD pulse-height data to measured average PD current. The relationship given in previous standards on PD measurement [27] is not generally correct.

## 6 References

- FRUTH, B., and NIEMEYER, L.: 'The importance of statistical characteristics of partial discharge data', *IEEE Trans.*, 1992, **EI-27**, pp. 60–69
- OKAMOTO, T., and TANAKA, T.: 'Novel partial discharge measurement computer-aided measurement systems', *IEEE Trans.*, 1986, **EI-21**, pp. 1015–1016
- VAN BRUNT, R.J.: 'Stochastic properties of partial-discharge phenomena', *IEEE Trans.*, 1991, **EI-26**, pp. 902–948
- KREUGER, F.H., GULSKI, E., and KRIVDA, A.: 'Classification of partial discharges', *IEEE Trans.*, 1993, **EI-28**, pp. 917–931
- FLORKOWSKA, B., and WLODEK, R.: 'Pulse height analysis of partial discharges in air', *IEEE Trans.*, 1993, **EI-28**, pp. 932–940
- ROBINSON, G.: 'Discharges in asymmetric cavities under AC stresses', *IEE Proc. A*, 1992, **27**, pp. 119–126
- GULSKI, E., and KREUGER, F.H.: 'Computer-aided recognition of discharge sources', *IEEE Trans.*, 1992, **EI-27**, pp. 82–92
- GULSKI, E., and KRIVDA, A.: 'Neural networks as a tool for recognition of partial discharges', *IEEE Trans.*, 1993, **EI-28**, pp. 984–1001
- SATISH, L., and GURVRAJ, B.I.: 'Use of hidden Markov models for partial discharge pattern classification', *IEEE Trans.*, 1993, **EI-28**, pp. 172–182
- KRANZ, H.-G.: 'Diagnosis of partial discharge signals using neural networks and minimum distance classification', *IEEE Trans.*, 1993, **EI-28**, pp. 1016–1024
- SUZUKI, H., and ENDOH, T.: 'Pattern recognition of partial discharge in XLPE cables using a neural network', *IEEE Trans.*, 1992, **EI-27**, pp. 543–549
- HOZUMI, N., OKAMOTO, T., and IMAJO, T.: 'Discrimination of partial discharge patterns using a neural network', *IEEE Trans.*, 1992, **EI-27**, pp. 550–555
- MASON, J.H.: 'Discharges', *IEEE Trans.*, 1978, **EI-13**, pp. 211–238
- TANAKA, T.: 'Internal partial discharge and material degradation', *IEEE Trans.*, 1988, **EI-21**, pp. 899–905
- HOZUMI, N., OKAMOTO, T., and FUKAGAWA, H.: 'Simultaneous measurement of microscopic image and discharge pulses at the moment of electrical tree initiation', *Jap. J. Appl. Phys.*, 1986, **27**, pp. 572–576
- ROGERS, E.C.: 'The self-extinction of gaseous discharges in cavities in dielectrics', *Proc. IEE*, 1958, **105A**, pp. 621–630
- HUDON, C., BARTNIKAS, R., and WERTHEIMER, M.R.: 'Spark-to-glow discharge transition due to increased surface conductivity on epoxy resin specimens', *IEEE Trans.*, 1993, **EI-28**, pp. 1–8
- MORSHUIS, P.H.F.: 'Partial discharge mechanisms'. PhD thesis, Delft University Press, Delft, The Netherlands, 1993
- ISHIDA, T., MIZUNO, Y., NAGO, M., and KOSAKI, M.: 'Computer aided partial discharge analysing system for detection of swarming pulsive microdischarges'. IEE conference proceedings 378, 1993, pp. 99–100
- VAN BRUNT, R.J., and CERNYAR, E.W.: 'Stochastic analysis of AC-generated partial discharge pulses from a Monte-Carlo simulation', 1992 annual report: conference on electrical insulation and dielectric phenomena, IEEE, NY, 1992, pp. 427–434
- VAN BRUNT, R.J., CERNYAR, E.W., and VON GLAHN, P.: 'Importance of unravelling memory propagation effects in interpreting data on partial discharge statistics', *IEEE Trans.*, 1993, **EI-28**, pp. 905–916
- VAN BRUNT, R.J., VON GLAHN, P., and LAS, T.: 'Partial discharge-induced ageing of cast epoxies and related nonstationary



- behaviour of the discharge statistics'. 1993 annual report: conference on electrical insulation and dielectric phenomena, IEEE, NY, 1993, pp. 455-461
- 23 VAN BRUNT, R.J., VON GLAHN, P., and LAS, T.: 'Nonstationary behaviour of partial discharge during insulation ageing'. IEE conference proceeding 378, 1993, pp. 29-30
  - 24 VAN BRUNT, R.J., and CERNYAR, E.W.: 'Influence of memory propagation on phase-resolved stochastic behaviour of AC-generated partial discharges', *Appl. Phys. Lett.*, 1991, **58**, pp. 2628-2630
  - 25 VAN BRUNT, R.J., CERNYAR, E.W., VON GLAHN, P., and LAS, T.: 'Variations in the stochastic behaviour of partial-discharge pulses with point-to-dielectric gap spacing'. Conference record: 1992 IEEE international symposium on electrical insulation, IEEE publ. 92CH3150.0, 1992, pp. 349-353
  - 26 VAN BRUNT, R.J., and CERNYAR, E.W.: 'System for measuring conditional amplitude, phase or time distributions of pulsating phenomena', *J. Res. Nat. Inst. Stand. Tech.*, 1992, **97**, pp. 635-672
  - 27 'Partial discharge measurements'. International Electrotechnical Commission, IEC Standard, Publ. 270, 1981, pp. 47
  - 28 VAN BRUNT, R.J., STRICKLETT, K.L., STEINER, J.P., and KULKARNI, S.V.: 'Recent advances in partial discharge measurement capabilities at NIST', *IEEE Trans.*, 1992, **EI-27**, pp. 114-129
  - 29 BARTNIKAS, R., and NOVAK, J.P.: 'On the character of different forms of partial discharge and their related terminologies', *IEEE Trans.*, 1993, **EI-18**, pp. 956-968
  - 30 VON GLAHN, P., and VAN BRUNT, R.J.: 'Performance evaluation of a new digital partial discharge recording and analysis system'. Conference record: 1994 IEEE international symposium on electrical insulation, Pittsburgh, 1994, pp. 12-16
  - 31 HUDON, C., BARTNIKAS, R., and WERTHEIMER, M.R.: 'Analysis of degradation products on epoxy surfaces subjected to pulse and glow-type discharges'. 1991 annual report' conference on electrical insulation and dielectric phenomena, IEEE, NY, 1991, pp. 237-243

## 7 Appendix

A brief description is given here of the modifications in the Monte-Carlo model of PD described by Van Brunt and Cernyar [20] that are required to simulate the effect of PD induced changes in dielectric surface conductivity. A decay of negative surface charge can be accommodated in the model by making an appropriate change in eqn. 12 of this reference which gives the time dependent local field at the discharge site and can be written in the form:

$$E(t) = E_0 \sin(2\pi ft) - \sum_{j=1}^N \left( \sum_i \Delta E_{ij}^+(t_{ij}^+) - \sum_k \Delta E_{kj}^-(t_{kj}^-) \right) \quad (11)$$

where the first term on the right-hand side corresponds to the sinusoidal applied field and the second term,

denoted below by  $\Delta E(t)$ , corresponds to the local field due to PD produced surface charge. In the second term  $\Delta E_{ij}^\pm$  is the field change due to the  $i$ th positive or negative PD pulse in the  $j$ th voltage cycle, assumed to occur at time  $t_{ij}^\pm$ , and  $N$  is the number of full cycles that have occurred up to time  $t$ . The local field strength after an incremental increase in time from  $t$  to  $t + \Delta t$  is given by:

$$E(t + \Delta t) = E_0 \sin[2\pi f(t + \Delta t)] - \Delta E(t + \Delta t) \quad (12)$$

where, if no PD event occurs in the time  $\Delta t$ ,

$$\Delta E(t + \Delta t) = \Delta E(t) \quad (13)$$

and if a discharge event occurs within  $\Delta t$ ,

$$\Delta E(t + \Delta t) = \Delta E(t) \mp \Delta E_{ij}^\pm \quad (14)$$

To allow for a negative surface-charge decay, we introduce a decay constant  $\gamma$ , assumed to be proportional to the dielectric surface conductivity. The calculation of the local field using eqn. 12 is then modified so that, if  $\Delta E(t) \leq 0$  and no PD event occurs in the time  $\Delta t$ ,

$$\Delta E(t + \Delta t) = \Delta E(t) \exp(-\gamma \Delta t) \quad (15)$$

Eqn. 13 still applies if  $\Delta E(t) > 0$  and eqn. 14 still applies if a PD event occurs in  $\Delta t$  independent of the sign of  $\Delta E(t)$ .

In our original model, the effective work function,  $\Phi^+$ , of the dielectric surface was assumed to be a constant (i.e. independent of the local field). To allow for a negative surface charge dependent initiation probability of positive PD, the effective work function of the dielectric surface is allowed to have the form:

$$\Phi^+(t) = a_0 - a_1 \left( \frac{\Delta E(t)}{E_0} \right) - a_2 \left( \frac{\Delta E(t)}{E_0} \right)^2 \quad (16)$$

for  $\Delta E(t) < 0$ , where  $a_0$ ,  $a_1$ , and  $a_2$  are positive adjustable constants, and it is assumed that  $\Delta E(t)$  is proportional to the surface charge deposited by the discharge events. It should be emphasised that both of the above modifications are necessary to account for a disappearance of positive PD. It was also found that the ageing effect observed here could be simulated by allowing the decay constant  $\gamma$  to increase in proportion to the net negative PD exposure as measured by the sum  $\sum_{i,j} \Delta E_{ij}^-$ . The authors plan to present a more detailed description of the modified Monte-Carlo simulator of PD in a future work.